Characterizing the Performance of an Eppley Normal Incident Pyrheliometer

Frank Vignola
Fuding Lin
Department of Physics
Department of Chemistry
1274-University of Oregon
Eugene, OR 97403-1274
fev@uoregon.edu
flin@uoregon.edu

ABSTRACT

An Eppley Normal Incident Pyrheliometer (NIP) is calibrated against an Eppley Hickey-Frieden Absolute Cavity Radiometer under a variety of environmental conditions on selected sunny days over a year. For the NIP under study, the standard deviation for all the calibration data is 0.34% or an uncertainty of 0.68% at the 95% confidence level. The absolute uncertainty of the NIP is about 1% when other factors, such as the absolute uncertainty of the cavity radiometer, are included. Correlations with various parameters can reduce the scatter of the calibration measurement by approximately 50%. It is postulated that the meteorological parameters induce systematic offsets that when accounted for could produce more accurate values of beam irradiance. A series of experiments were conducted to evaluate the physical basis of the correlation. Evaluation of the experiments leads to some conclusions and suggestions for future tests.

1. INTRODUCTION

With interest growing in the deployment of solar energy system, the accuracy of irradiance measurements becomes increasingly important. Precise measurement of direct normal irradiance (DNI) is especially crucial for concentrating solar energy systems. The Eppley Normal Incident Pyrheliometer (NIP) is used extensively for DNI measurements as it has excellent stability [1] and is capable of producing DNI values with an accuracy of ±2%. It may be possible to improve on the accuracy of these values if parameters that affect the performance of the NIP can be identify and used to remove "systematic" errors in the measurements.

A preliminary study of parameters that affect the NIP performance was published earlier [2]. However, only 9 months with calibration results were available for the study and none of the calibrations were performed during the summer when higher temperatures were expected to affect the calibrations. Approximately 15 months of data are used in this study and the larger data set confirms some of the earlier findings and also illustrates the dependence on temperature.

So many environmental parameters affect the responsivity of the NIP, such as relative humidity, temperature, and air mass, that study is warranted to better understand how these factors interact when they influence the NIP's responsivity. Therefore, we conducted a series of tests with thermocouples applied to the body of the NIP to study how the heat flow could affect the NIP's responsivity. The tests and correlations do lead to some conclusions, but further tests and correlation results are needed to establish reliable results that can be used with confidence.

In this paper the correlations with various parameters are obtained and evaluated. Three correlations are evaluated, including one which incorporates pyrgeometer measurements not normally available at many sites. Next the experiments in heat flow on the NIP are described and the results of the finding are presented. The results are then discussed and summarized and future tests are suggested.

2. CALIBRATION OF THE NIP

Beginning in the fall of 2009, calibrations using a Hickey-Frieden Absolute Cavity Radiometer (AHF) were conducted at the University of Oregon in Eugene, Oregon. The station NIP has been in operation during the period in which about

a dozen calibrations have been run. This paper uses the data gathered during these runs to characterize the performance of the NIP under different environmental conditions. All the periods were sunny and periods with clouds were excluded.

The NIP is mounted on an automatic tracker that keeps the instrument aligned with the sun. The NIP was initially connected to a Campbell CR10x data logger, and later, a CR 1000 data logger and it is scanned every two seconds. The one minute averages are then stored in memory to be retrieved later in the day. Starting in July 2010, twenty-second samples were gathered for the NIP and other meteorological data to correspond with the data being gathered with the AHF.

The AHF is mounted on the tracker opposite the NIP so the alignment of the two instruments should be the same. The AHF consists of a balanced cavity receiver pair attached to a wire-wound and plated thermopile. The blackened cavity receivers are fitted with heater windings which allow for absolute operation using the electrical substitution method, which relates radiant power to electrical power. The forward cavity views the direct beam irradiance through a precision aperture having a 5° field of view. The rear receiver views an ambient temperature blackbody [3]. The control box for the AHF was modified to use the software program developed by the National Renewable Energy Laboratory (NREL), a different relay board, and a 1 ohm resistor in place of the 10 ohm resistor usually employed.

The AHF used in this study has its calibration traceable to the international standard through a pyrheliometer inter-comparison against a reference AHF at NREL. The NREL AHF is used in the international pyrheliometer inter-comparison that sets the international calibration standard, and therefore, instruments calibrated at NREL have their calibration traceable to the international standard.

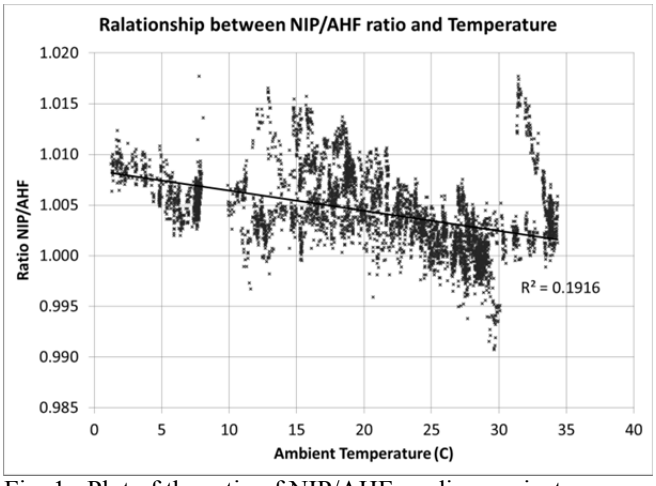

Fig. 1: Plot of the ratio of NIP/AHF reading against temperature. The R^2 for the linear fit is 0.19.

The AHF and associated electronics are connected to a National Instruments GPIB ExpressCard that is plugged into a laptop computer to record and format the reference beam data. The AHF is calibrated before and after each 12-minute run and data are collected every 20 seconds. This is the method used at the pyrheliometer inter-comparison and it was used to check the calibration of the AHF.

Eppley Labs lists the NIP characteristics as follows:

- Sensitivity: approx. 8 $\mu V/Wm^{-2}$.
- Impedance: approx. 200 Ohms.
- Temperature Dependence: ±1% over ambient temperature range -20 to +40°C.
- Linearity: ±0.5% from 0 to 1400 Wm^{-2}.
- Response time: 1 second (1/e signal).

The response time for the AHF is on the order of 2 seconds and is similar to that of the NIP. The absolute accuracy of the AHF is better than 0.5%.

The AHF and NIP were compared on six clear day periods from October 8, 2009 to July 6, 2010 using one minute average data and six clear days from July 14, 2010 to February 1, 2011 using 20 second data.

3. CORRELATING AHF DATA WITH NIP AND METEOROLOGICAL DATA

In a previous paper [2] the responsivity of the NIP was studied using data from six clear days. The data were limited to fall, winter, and spring. With this shorter dataset, it was found that the NIP responsivity correlated with DNI irradiance, wind speed, zenith angle, air mass, and atmospheric pressure. No correlations with temperature and relative humidity were found and it was postulated that the range of temperature and relative humidity values in the summer would extend the range of parameters under study, and a dependence on temperature, at least, was expected.

The nominal responsivity used for the NIP under study is 8.12 $\mu V/Wm^{-2}$. The W/m^2 output of the NIP is the voltage reading of the NIP divided by its nominal responsivity. The method chosen to examine the responsivity of the NIP consists of dividing the NIP irradiance by that measured by the AHF. If the NIP/AHF ratio is greater than 1.0 then the actual responsivity is higher than the nominal responsivity.

The ratio between the NIP readings and the AHF cavity values against temperature is shown in Fig. 1. The trend line for this plot has an R^2 value of 0.19 indicating that there is some temperature dependence in the responsivity of the NIP. It is not clear why a group of readings that occurs between 33 and 35 °C appears higher than expected. These reading occurred during a single day. It would be worthwhile to get more data from similar days.

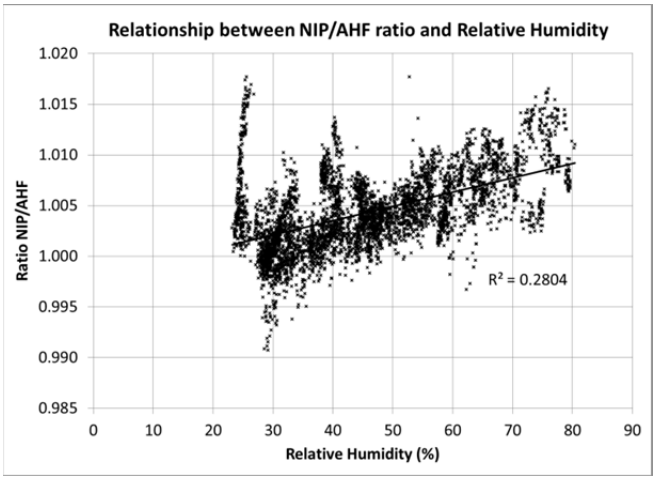

Fig. 2: Plot showing the relationship between relative humidity and the ratio of the NIP and AHF readings. The R^2 value is 0.28 indicating that there is a strong correlation.

The term R^2 is the ratio of the sum of the squares of errors divided by sum of the squares of the total variation. The sum of the squares of error is the sum of the difference between the predicted value and the actual value squared. The sum of squares of the total variation is the sum of the value from the average value squared. R^2 can be considered the percentage of the variation explained by the regression fit. Therefore the larger R^2 the better the regression fit.

A plot of relative humidity verses the NIP/AHF ratio is shown in Fig. 2. Note that there is a strong correlation between relative humidity (R^2 is 0.28). That is on the clear days used in this study there is a strong correlation between temperature and relative humidity, the higher the temperature the lower the relative humidity tends to be.

Many of the meteorological and other parameters that correlate individually with the NIP/AHF ratio also correlate well with each other. Ideally, in a multivariate regression, the variable should be independent. Here, many of the measured variables are related, and it is difficult to determine the which variable physically causes changes in the NIP's responsivity.

Table 1 contains variables whose correlation with the NIP/AHF ratio has been studied. The standard error is 0.0022 and R^2 is 0.68. These variables explain about two thirds of the variation between the measured NIP/AHF ratio and the estimate ratio. The zenith angle is the least well correlated variable.

Possibly, other factors are also involved. It was suggested that the change in wind speed might be salient [4]. The regression analysis was repeated, this time including the change in wind speed as a parameter (Table 2). In this case, the standard error is 0.0025 and R^2 is 0.72. However, there were fewer days with data here than in the case without the change in wind speed parameter.

TABLE 1: MULTIVARIATE CORRELATION WITH NIP/AHF

Variable	*Coefficients*	*Standard Error %*
Intercept	12.4951515029	5.65%
Wind Speed	-0.0018120977	5.21%
Wind Speed squared	0.0001816977	9.51%
Atmospheric Pressure	-0.0228575339	6.20%
Atmospheric Pressure Squared	0.0000113968	6.24%
DNI	-0.0000456908	6.92%
DNI squared	0.0000000193	10.24%
Ambient Temperature	-0.0002034019	7.65%
Air mass, pressure-corrected	-0.0007850196	12.42%
Relative Humidity	0.0000274469	17.36%
Zenith Angle	0.0000199672	26.35%

TABLE 2: ALTERNATIVE MULTIVARIATE CORRELATION WITH NIP/AHF

Variable	*Coefficients*	*Standard Error %*
Intercept	4.334971057	19.49%
Ambient Temperature	-0.000504287	4.00%
DNI	-6.35817E-05	4.69%
DNI Squared	2.40932E-08	6.65%
Wind Speed	-0.001817899	5.10%
Wind Speed Squared	0.00019391	8.84%
Air mass, pressure-corrected	-0.001839425	5.84%
Relative Humidity	-4.94614E-05	12.18%
Change in Wind Speed	-0.000315988	15.54%
Atmospheric Pressure	-0.006320393	26.91%
Atmospheric Pressure Squared	3.04502E-06	28.08%

Examining the two regression results shows that the relative importance of the various variables change when the parameters change. This results from interdependence of the variables and the limited amount of data available for the analysis.

In addition to the meteorological variables measured at the Eugene station, pyrgeometer measurements commenced. The pyrgeometer produces measurements of download long wavelength flux (DWLong), IR flux from the detector (or Detector Flux – DF), and the temperatures of the body and dome of the pyrgeometer. The sky brightness temperature is equal to $(DWLong/Sigma)^{1/4}$, where sigma is the Stefan-Boltzman constant 5.6704×10^{-8} W m^{-2} K^{-4}. K is temperature in kelvins.

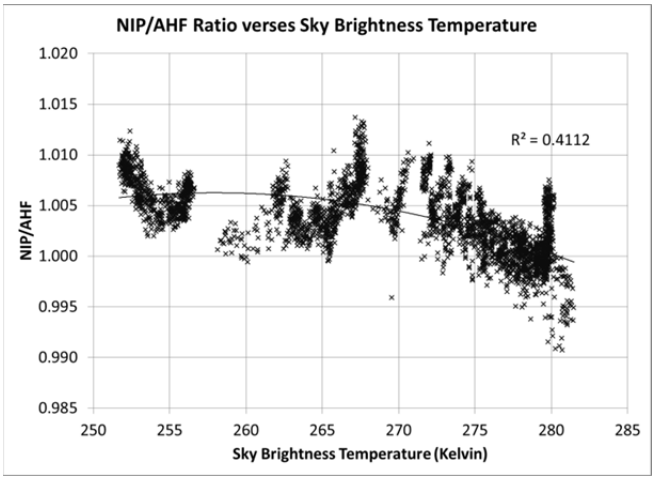

Fig. 3: Plot of NIP/AHF ratio verses the sky brightness temperature. R^2 is 0.41.

The sky brightness temperature as determined from the pyrgeometer data is plotted against the NIP/AHF ratio in Fig. 3. The R^2 value of the regression fit to the data is 0.41. This value is larger than found with most of the other variables used in the regression fit.

A multivariate regression was then performed with the data from the pyrgeometer. The results are shown in Table 3. A quadratic formula worked best for the regression and the air mass parameter had the smallest standard error. For this regression, the standard error was 0.0015 and the R^2 was 0.82. This is a substantial improvement over the previous regressions, but, of course, it required pyrgeometer data to obtain the better results. Note that the change in wind speed variable was not included in this correlation because it did not reduce the standard error.

From the three examples shown, it is evident that there are many ways to correlate meteorological parameters with the NIP's responsivity. However, it is uncertain which parameters are tied directly to the change in the NIP's responsivity and which are only indirectly related. Both more data and a better understand of how the NIP responds to thermal fluxes are needed before an algorithm can be developed to correct the small systematic errors in the NIP readings.

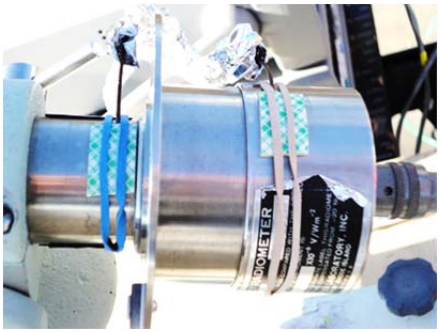

Fig. 4: Photo showing outdoor experimental setup.

TABLE 3: MULTIVARIATE CORRELATION INCLUDING SKY BRIGHTNESS TEMPERATURE

Variable	*Coefficients*	*Standard Error %*
Intercept	322.1657195	14.99%
Air mass, pc	0.003798653	3.95%
Air mass squared	-0.00030659	6.36%
Ambient Temperature	0.001154922	7.16%
Relative Humidity	0.000157801	7.40%
Wind Speed	-0.000642915	12.41%
Wind Speed Squared	5.19749E-05	26.11%
Sky Temperature	-4.881062763	15.08%
Sky Temp Squared	0.026815817	15.44%
Sky Temp Cubed	-6.53968E-05	15.83%
Sky Temp Fourth	5.97237E-08	16.25%
Air Pressure	0.02258298	34.53%
Air Pressure Squared	-1.09572E-05	35.67%

4. TESTING THE NIP'S THERMAL PATHWAYS

There are a variety of ways that external influences might affect the performance of the NIP. In order to determine the magnitude and nature of these influences, it was decided to look at how heat applied to the NIP would affect the NIP readings. At a meeting in August 2010, the NREL Solar Radiation Research Laboratory team said that a dark NIP offset of up to ±40 W/m^2 could be induced by creating a temperature gradient between the NIP body (tube) and its base with the heat from the hand holding the NIP. We decided to reproduce the result independently and to perform other experiments to study the effects of external heat flow by monitoring the temperature difference (ΔT) between the body of the NIP and the base. Two thermocouples were used and the ΔT was correlated with the NIP dark offset. The dark offset refers to the pyrheliometer reading when the window of the NIP is covered and no light is allowed to enter.

4.1 Experimental Details

For both indoor and outdoor experiments, two K-type fast response (flattened junction) thermocouples were attached to the NIP. One thermocouple was attached to the narrow NIP body tube just in front of the end flange and the second thermocouple was attached to the surface alongside the specification plate, about 1 inch from the base of the NIP (Fig. 4). Thermocouples were wired such that a positive voltage was produced if the temperature of the narrow tube was higher than that of the base. Aluminum foil was used to shield the wires of both thermocouple wires from sunlight and EM interference.

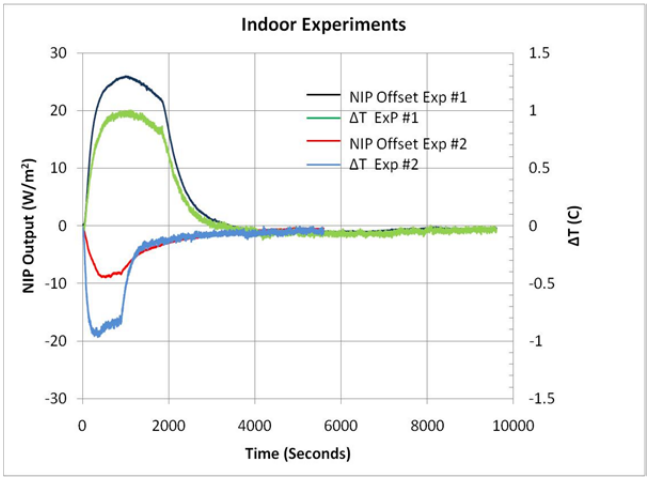

Fig. 5: Changes in NIP output and temperature difference between the two thermocouples when a heat flow is induced by holding either the NIP body tube or the base. Warming only the narrow body tube with the hand produces a positive NIP output offset (black line) as well as a positive temperature difference (green line). The opposite happens when only the NIP's base is warmed by the hand.

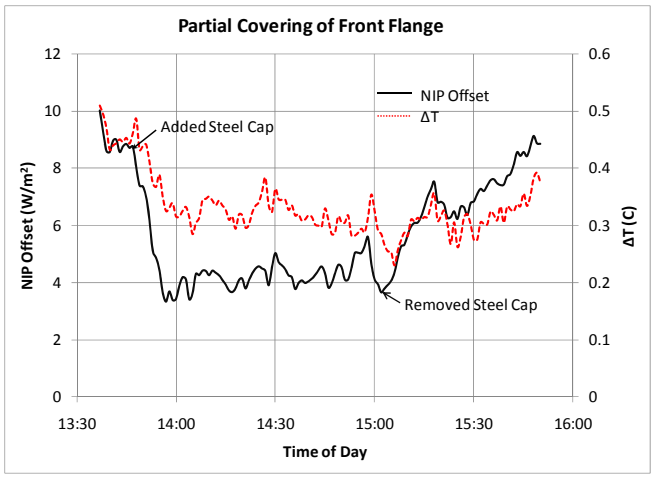

Fig. 6: Plot of the temperature difference between two thermocouples and the output of the NIP with its window covered with partial shading of the front flange. The solid line is the NIP offset. The dashed line is the temperature difference between the two thermocouples.

For indoor experiments, the NIP was seated on a piece of closed-cell insulating foam without any clamping. For outdoor experiments, the NIP was clamped to an Eppley ST1 tracker. The encircling clamp contacted the NIP's narrow body at about 1.5 inches in front of the end flange.

The voltage from the pair of thermocouples was measured by an Agilent 34411A multimeter, while the NIP output voltage was measured by an Agilent 34410A multimeter. Both signals were recorded to a PC with a custom LabView program. Any imperfection in the electrical connections may result in an offset of the thermocouple pair's output voltage.

4.2 Observations from Indoor Experiment

The indoor experiment is a non-natural circumstance and is only useful for learning about heat flow. In experiment #1 the hand held the NIP by the tube in front of the back flange. In experiment #2 the hand held the base end of the NIP. Figure 5 shows the results of the experiments.

The following conclusions were reached.

1. The sign of the NIP output was always the same as the sign of ΔT when a heat flow was induced. The changes in both curves correlate very well.
2. Although warming only the base resulted in a maximum ΔT comparable to that found when warming only the body tube, the maximum NIP negative output resulting from warming only the base was 1/3 of that resulting when only the body tube was warmed.
3. After the heat source was taken away from the tube in front of the flange, both the NIP output and ΔT continued to decrease until they overshot to negative values. This overshoot was not observed when warming only the base.

4.3 Observations from the Outdoor Experiment

While testing the NIP under controlled conditions in the laboratory can provide insights into performance changes caused by temperature differentials, it is the performance outdoors under operational conditions that needs to be understood. In the following series of outdoor experiments, both the ΔT signal and NIP output signal were measured. The signals were much noisier than during the experiment in the laboratory even after careful shielding of the connecting cables. The NIP and ΔT outputs signals were sampled every second and were averaged to one minute to make the comparisons easier to visualize.

First, the effect of partially shading the front flange was observed. Initially only the glass window was covered. An aluminum cap on top of a 2-mm-thick black neoprene layer was used for this purpose. Then at 13:43, an additional stainless steel cap of r =1.5 inches, covering about half of the front flange area, was installed. The stainless steel cap was removed at 15:03. The results of the experiment are shown in Fig. 6.

4.3.1 Evaluation of Partial Shading of Front Flange

The following behavior was observed during the flange shading experiment (see Fig. 6).

1. The NIP produces a positive output even when the window is covered. The magnitude of NIP output decreases when a greater portion of the front flange was shaded.

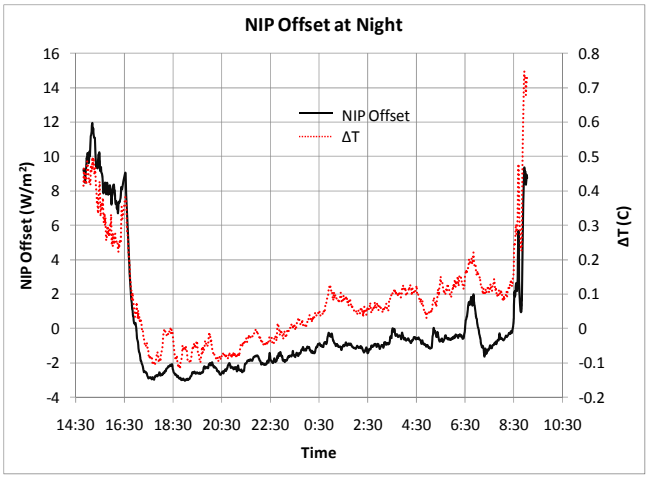

Fig. 7: Changes in temperature differential between two thermocouples and the output of the covered NIP from before sunset on 2/02/2011 to the morning of 2/03/2011. At sunset, the NIP was rotated to point up at a 30 degree angle facing due south.

2. On average, the changes in NIP output offset correlates well with the changes in ΔT.

4.3.2 NIP Pointing Upward Overnight

Nighttime readings can be very useful. In general thermopile pyranometers, used for global horizontal irradiance (GHI) measurement, exhibit negative nighttime readings because the black disc in the pyranometer radiates to the night sky and this creates a temperature difference between the body of the pyranometer connected to the cold side of the thermopile and the disc that is directly connected to the "hot" side of the thermopile. There is probably is some IR radiative loss from the NIP, but the window sees only a 5.7° portion of the sky, so the IR radiative loss through the window will be very small.

However, nighttime reading can show behavior that is difficult to see during the day when the heat of the sun dwarfs many smaller effects. In this experiment, the NIP was rotated after sunset to point up at a 30° angle facing due south and it remained in that position until the next morning. The data from this experiment is plotted in Fig. 7.

The following observations were made after examining the data:

1. Overall, the changes in NIP output still follows the changes in ΔT.
2. After sunset, the NIP output signal overshoot to negative values and slowly returned to near zero throughout the night.
3. The ΔT changed sign after sunset and slowly returned to positive values.

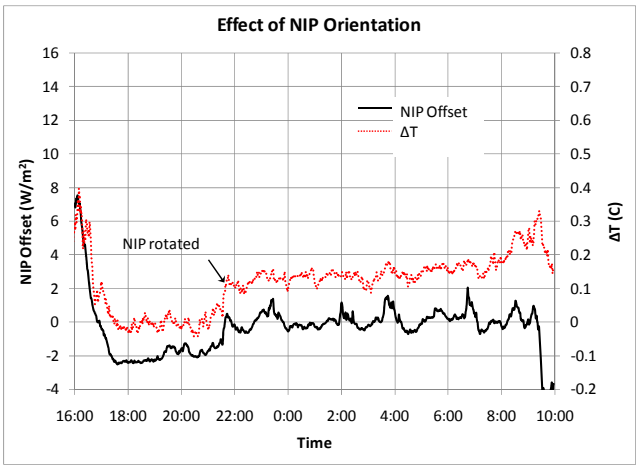

Fig. 8: Changes in temperature differential between two thermocouples and the output of the covered NIP from before sunset on 2/03/2011 to the morning of 2/04/2011. The NIP was left at pointing southwest (near horizontal) after sunset. At 21:37 the NIP was rotated so that it was pointed down 30 degrees facing due north.

4.3.3 NIP Pointing to Ground Overnight

During another nighttime experiment, the tracker was turned off a sunset when the NIP was horizontal. At 21:37 it was rotated by 30° so that the window of the NIP was facing the ground. It was left in this position for the rest of the night. A plot of the data is shown in Fig. 8.

The following observations were made after examining the data.

1. Overall, the changes in NIP output still follow the changes in ΔT.
2. After sunset and before 21:37 the NIP output signal overshot to negative values then slowly trended back to zero.
3. The ΔT was zero when the NIP was horizontal.
4. After the NIP was rotated so that the window faced the ground, the NIP output fluctuated around zero throughout the night until the morning sunlight induced a large negative output.

5. DISCUSSION AND CONCLUSIONS

Details of heat flow pathways within the instrument are important for understanding how changes in the environment can affect the responsivity of the instrument since the NIP output voltage is ultimately determined by the temperature difference between the hot and cold junctions inside the instrument. Without knowing the details of the internal thermal pathway design, one could only hypothesize based on the observations.

The indoor testing results shown in Fig. 5 indicate that the thermal pathway from the NIP tube to the internal hot junction is shorter than that from the tube to the internal cold junction. The tests also indicate that the thermal pathway from the base of the NIP to the cold junction is shorter than that to the hot junction.

The overshoot that occurs during the cooling phase of indoor experiment #1, and the absence of it during the cooling phase of indoor experiment #2 is consistent with the fact that the base of the NIP has a significantly larger thermal mass than the thinner body tube. The negative NIP output after sunset, which was observed during outdoor experiments could also be explained by the thermal mass difference between the NIP body tube and base. When the heat source (sunlight) disappears, then the front-to-back heat flow gradually slows to a stop and reverses direction since the environment cools the tube faster than the heavy base and leads to a negative NIP output (Figures 7 and 8).

When sunlight heats the front flange it generates a heat flow from the NIP body tube to the base of the NIP. A positive NIP offset voltage is created along with a positive ΔT between the two thermocouples. The magnitude of both signals decreases when a greater portion of the front flange is shaded so that the heat flow through the NIP body to the base is reduced.

The heat generated at the front flange can flow to the hot side of the thermal pile junction either through conduction or radiation. The measured ΔT reflects the thermal gradient due to conduction. The contribution from radiative heat transfer can be tested indoor by putting a good heat sink at the middle of the body tube to cut out the conduction and determine whether an increase of temperature in the front flange still produces a positive NIP output voltage.

Observations from the outdoor experiment, in which the NIP was rotated to point downward during the night, suggest that the temperature difference between ground and night sky could contributes approximately 2 W/m^2 to the dark offset of the NIP.

The observations from indoor and outdoor heat flow experiments alone, however, cannot explain why the actual responsivity of the NIP decreases with increasing solar irradiance as shown by a typical calibration curve plotted against time of day (the "smiley face" shape). Indeed the opposite would have been consistent since the front-to-back heat flow would be stronger with higher solar irradiance. Therefore, there must be other dominating factors that lead to the "smiley face" calibration curve.

Our conjecture is that the NIP does not precisely compensate for any imperfections in the thermal grounding. Imperfect thermal grounding here refers to both the inadequate heat dissipation from the cold junction to the thermal ground (NIP base), and the thermal leakage from the hot junction to the thermal ground.

Since the output voltage of the NIP is determined by the temperature difference (ΔT) between the hot and cold junctions inside the instrument, both inadequate heat dissipation from the cold junction and thermal leakage from the hot junction to thermal ground will have similar effect of reducing ΔT, therefore reducing the actual responsivity of the NIP. It is logical to expect that the effect of imperfect thermal grounding would be more pronounced when the hot junction temperature is higher during periods of high solar irradiance and less noticeable when the solar irradiance is low. This would explain the "smiley face" shape of the calibration curve.

The correlation between the NIP/AHF ratio and other meteorological data may also be explained by an imperfect thermal grounding. Both lower air temperature and higher relative humidity could lead to more efficient dissipation of heat from the NIP, i.e. better thermal grounding, and therefore higher true responsivity of the NIP.

However, the effect of wind speed on the NIP responsivity is more complicated. On the one hand, higher constant wind speed will improve thermal grounding thus increasing the NIP responsivity. On the other hand, an increase in wind speed will also cool down the NIP body tube quicker than the base, reducing the NIP responsivity. Because wind speed is constantly changing, its net effect on NIP responsivity is less clear.

The higher the sky brightness temperature, the lower the responsivity. This relationship indicates that there is an IR radiative pathway that affects the NIP readings. The exact nature of this pathway has not been determined.

The observation that the NIP offset was zero when the NIP was in a horizontal position is interesting. The offset is similar, although small, when the NIP faces up or down at an angle of 30°. The night the NIP window faced up did seem to take longer to reach thermal equilibrium, but that is only one evenings' worth of observations. Although the magnitude of the difference between the NIP on a tilt verses a horizontal orientation is only on the order of 1 to 2 W/m^2. Tilt could be one of many factors affecting the NIP responsivity.

6. SUMMARY AND FUTURE DIRECTIONS

Many factors affect the performance of the Eppley NIP. The influence of each of these factors appears small and some of the effects seem to be countered by other effects. Because there are many factors that can affect the NIP's

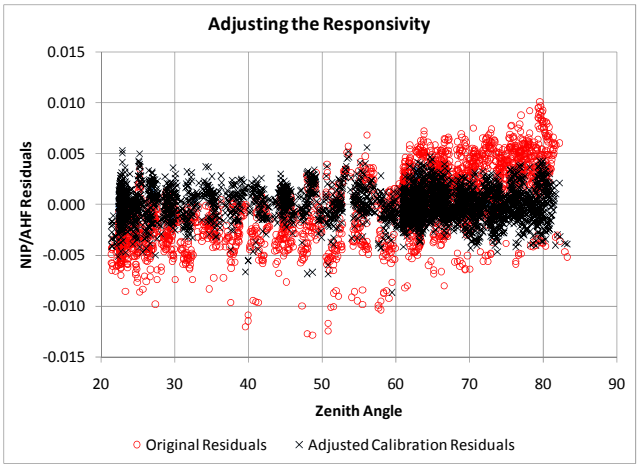

Fig. 9: Comparison of residuals from the original NIP/AHF ratio to residuals after the regression adjustment (Table 3). The residuals from the original calibrations are plotted as red circles. The residuals of the adjusted calibration are plotted as black x's.

performance, regression analysis is complex. Of the three analyses presented in this paper, the regression using the sky brightness temperature gave the best results. A summary of effect of various parameters on the responsivity is given in Table 4.

While there are systematic errors in the calibration, these errors are small. Twice the standard error (95% certainly level) of the original calibrations was 0.68%. An error percentage of 0.68% represents error of between 4 and 7 W/m^2. The absolute accuracy is near 1% because other factors such as the absolute accuracy of the AHF have to be taken into account (about 0.45%). Twice the standard error for the adjusted calibrations is only 0.33%.

A plot of the residuals from the correlation with parameters in Table 3 are shown in Fig. 9 illustrates the improvements that is possible. This plot is for a single NIP and may not be representative of all NIPs or the performance of the NIP at a different location. In a previous paper [2], it was found that the spectral change irradiance could result in between 0.1 and 0.2% percent change in the responsivity value obtained. This also means that spectral differences over the year or from location to location could affect the NIP readings or calibration determination.

The correlation with the sky brightness temperature is interesting. The sky brightness temperature differs between Golden, Colorado and Eugene, Oregon. The NIP calibrated in Eugene was also calibrated in Golden. It appears that the Golden calibration showed a larger variation in responsivity over the day than in Eugene. The sky temperature was a factor in the difference in pyranometer calibrations between instruments calibrated in Eugene and at Golden. The difference in the NIP calibrations is much smaller, but

TABLE 4: FACTORS AFFECTING RESPONSIVITY

Factor	Actual responsivity compared to nominal responsivity with an increase of factor
Calibrations Results	Actual Responsivity higher near noon
Wind Speed	Actual responsivity decreases
Heating Front Flange	Actual responsivity increases
DNI	Actual responsivity decreases
Air Mass	Actual responsivity increases
Ambient Temperature	Actual responsivity decreases
Zenith Angle	Actual responsivity increases
Relative Humidity	Actual responsivity increases
Sky Brightness Temperature	Actual responsivity decreases
Spectral Change Over the Day	Actual responsivity decreases
Orientation (Tilt)	Actual responsivity increases

perhaps, the difference in sky brightness temperature may play a role in NIP calibrations as well. The effect of sky brightness temperature bears further examination.

The interrelationships among the factors affecting the responsivity make the exact characterization of any particular affect difficult. More measurements under a variety of conditions are needed. This should include measurements at different locations.

7. AKNOWLEDGMENTS

The sponsors of the University of Oregon Solar Radiation Monitoring Laboratory should be acknowledged for support of our efforts to build a high quality solar radiation database in the Pacific Northwest. The sponsors are, the Bonneville Power Administration, National Renewable Energy Laboratory under NFE-8-88401-01, Energy Trust of Oregon, Eugene Water and Electric Board, Oregon Best, Emerald People's Utility District, and the Meyer Family Trust.

8. REFERENCES

(1) Laura Riihimaki and F. Vignola Trends in Direct Normal Solar Irradiance in Oregon from 1979-2003 *Proc. Solar World Congress, International Solar Energy Society,* 2005
(2) F. Vignola and Fuding Lin, Evaluating calibrations of normal incident pyrheliometers, Proceedings of SPIE, Volume 7773, 2010
(3) http://www.eppleylab.com/
(4) Private communications with Steve Wilcox of NREL.